

Cross Sections and Beam Asymmetries for $K^+\Sigma^{*-}$ photoproduction from the deuteron at $E_\gamma = 1.5\text{-}2.4 \text{ GeV}$

K. Hicks,¹ D. Keller,¹ H. Kohri,² D.S. Ahn,^{2,3} J.K. Ahn,³ H. Akimune,⁴ Y. Asano,⁵ W.C. Chang,⁶ S. Daté,⁷ H. Ejiri,^{2,7} S. Fukui,⁸ H. Fujimura,^{9,10} M. Fujiwara,^{2,5} S. Hasegawa,² T. Hotta,² K. Imai,¹⁰ T. Ishikawa,¹¹ T. Iwata,¹² Y. Kato,² H. Kawai,¹³ Z.Y. Kim,⁹ K. Kino,² N. Kumagai,⁷ S. Makino,¹⁴ T. Matsuda,¹⁵ T. Matsumura,^{2,7} N. Matsuoka,² T. Mibe,^{2,1} M. Miyabe,¹⁰ Y. Miyachi,¹⁶ M. Morita,² N. Muramatsu,^{7,2} T. Nakano,² M. Niiyama,¹⁰ M. Nomachi,¹⁷ Y. Oh,¹⁸ Y. Ohashi,⁷ H. Ohkuma,⁷ T. Ooba,¹³ J. Parker,¹⁰ C. Rangacharyulu,¹⁹ A. Sakaguchi,¹⁷ T. Sasaki,¹⁰ P.M. Shagin,²⁰ Y. Shiino,¹³ A. Shimizu,² H. Shimizu,¹¹ Y. Sugaya,¹⁷ M. Sumihama,^{17,7} Y. Toi,¹⁵ H. Toyokawa,⁷ A. Wakai,²¹ C.W. Wang,⁶ S.C. Wang,⁶ K. Yonehara,⁴ T. Yorita,^{2,7} M. Yoshimura,²² M. Yosoi,^{10,2} and R.G.T. Zegers²³

(The LEPS Collaboration)

¹Department of Physics and Astronomy, Ohio University, Athens, Ohio 45701, USA

²Research Center for Nuclear Physics, Osaka University, Ibaraki, Osaka 567-0047, Japan

³Department of Physics, Pusan National University, Busan 609-735, Korea

⁴Department of Physics, Konan University, Kobe, Hyogo 658-8501, Japan

⁵Kansai Photon Science Institute, Japan Atomic Energy Agency, Kizu, Kyoto 619-0215, Japan

⁶Institute of Physics, Academia Sinica, Taipei, Taiwan 11529, Republic of China

⁷Japan Synchrotron Radiation Research Institute, Mikazuki, Hyogo 679-5198, Japan

⁸Department of Physics and Astronomy, Nagoya University, Nagoya, Aichi 464-8602, Japan

⁹School of Physics, Seoul National University, Seoul 151-747, Korea

¹⁰Department of Physics, Kyoto University, Kyoto 606-8502, Japan

¹¹Laboratory of Nuclear Science, Tohoku University, Sendai, Miyagi 982-0826, Japan

¹²Department of Physics, Yamagata University, Yamagata 990-8560, Japan

¹³Department of Physics, Chiba University, Chiba 263-8522, Japan

¹⁴Wakayama Medical College, Wakayama 641-8509, Japan

¹⁵Department of Applied Physics, Miyazaki University, Miyazaki 889-2192, Japan

¹⁶Department of Physics, Tokyo Institute of Technology, Tokyo 152-8551, Japan

¹⁷Department of Physics, Osaka University, Toyonaka, Osaka 560-0043, Japan

¹⁸Cyclotron Institute and Physics Department, Texas A&M University, College Station, Texas, 77843, USA

¹⁹Department of Physics, University of Saskatchewan, Saskatoon, Saskatchewan, Canada

²⁰School of Physics and Astronomy, University of Minnesota, Minneapolis, Minnesota 55455, USA

²¹Akita Research Institute of Brain and Blood Vessels, Akita 010-0874, Japan

²²Institute for Protein Research, Osaka University, Suita, Osaka 565-0871, Japan

²³NSCL, Department of Physics and Astronomy, Michigan State University, East Lansing, MI 48824, USA

(Dated: December 3, 2008)

The $\Sigma(1385)$ resonance, or Σ^* , is well-known as part of the standard baryon decuplet with spin $J = 3/2$. Measurements of the reaction $\gamma p \rightarrow K^+ \Sigma^{*0}$ are difficult to extract due to overlap with the nearby $\Lambda(1405)$ resonance. However, the reaction $\gamma n \rightarrow K^+ \Sigma^{*-}$ has no overlap with the $\Lambda(1405)$ due to its charge. Here we report the first measurement of cross sections and beam asymmetries for photoproduction of the Σ^{*-} from a deuteron target, where the K^+ and π^- are detected in the LEPS spectrometer. The cross sections at forward angles range from 0.4 to 1.2 μb , with a broad maximum near $E_\gamma \simeq 1.8 \text{ GeV}$. The beam asymmetries are negative, in contrast to positive values for the $\gamma n \rightarrow K^+ \Sigma^-$ reaction.

PACS numbers: 13.60.Rj, 13.88.+e, 24.70.+s, 25.20.Lj

The photoproduction of the spin $J = 3/2$ baryon resonance with strangeness -1 at a mass of 1385 MeV, known as the Σ^* , is virtually unknown except for a few early bubble-chamber experiments [1], preliminary data from CLAS [2], and data from LEPS with large photon energy bins [3] (all from a proton target). The Σ^* is the lowest mass strange baryon in the decuplet of $J = 3/2$ baryons, so measurements of its production cross section and spin observables are of intrinsic interest to compare with theoretical calculations based on SU(3) symmetry and the well known Δ resonance photoproduction amplitudes [4].

A recent paper by Oh, Ko and Nakayama [5] states “photoproduction of $K\Sigma^*$ provides a useful tool for testing baryon models”. In particular, the $K\Sigma^*$ final state, produced at higher W than for ground-state $K\Lambda$ or $K\Sigma$ production, may be a good way to search for the so-called “missing” resonances (those not listed by the Particle Data Group [6]) as predicted by the constituent quark model [7]. For example, Döring *et al.* [8] suggest that the $\Delta(1700)$ resonance may have a large coupling to the $K\Sigma^*$ channel. There are many measurements of Δ production, due to its strong production cross section, but

this does not give information on the $K\Sigma^*$ coupling.

Comparison between data for $K\Sigma^*$ production and reaction models is one way to search for new resonances. For example, in Ref. [5], preliminary data [2] for the reaction $\gamma p \rightarrow K^+\Sigma^{*0}$ near threshold are better fitted, within this effective Lagrangian model, with the addition of several high-mass resonances (see [5] for details). However, a larger body of data including spin asymmetry observables is needed before any conclusions can be reached on the need for additional baryon resonances.

Precise data for photoproduction of the Σ^* resonance will also help to constrain the SU(3) relations in production mechanisms of decuplet baryons. In the model of Ref. [5], many coupling constants are not constrained by data, so standard SU(3) flavor symmetry relations [6] were used for these coupling constants (*e.g.* those relating the $\pi N\Delta$ and $KN\Sigma^*$ couplings). The magnitude of SU(3) flavor symmetry breaking in decuplet baryon production is most easily tested by comparing theoretical models with data for both Δ and Σ^* photoproduction. As mentioned above, little data is available for production of decuplet baryons beyond the Δ , leaving SU(3) flavor symmetry largely untested among these baryons.

Here we report on the first photoproduction measurement of the $K^+\Sigma^{*-}$ final state, done at the SPring-8 facility with the LEPS detector [9] and a deuterium target. Both the K^+ and a coincident π^- (from the strong decay $\Sigma^{*-} \rightarrow \pi^-\Lambda$) were detected. Photons in the energy range of 1.5 to 2.4 GeV were produced using Compton backscattering of polarized laser light from 8 GeV electrons in the SPring-8 storage ring. Details of the beam and detectors have been described previously [9]. Briefly, the photon beam is incident on a 16 cm liquid deuterium target, followed by a scintillator called the start counter (SC) and a Cerenkov detector to veto e^+e^- pairs. Charged particles go through tracking detectors, into a dipole magnet, through wire chambers and on to a time-of-flight (TOF) scintillator wall placed 4 m from the target. The photon energy is calculated from the struck electron, which goes into a tagging spectrometer inside the SPring-8 storage ring. The trigger is formed from a tagged electron, the SC with no Cerenkov veto, and a hit in the TOF wall. The TOF resolution was about 150 ps, and the typical momentum resolution was 6 MeV/c at a momentum of 1 GeV/c.

The Σ^* was identified using the missing mass technique. The K^+ missing mass, $MM(K^+)$, is selected between 1.325 and 1.445 GeV to isolate the Σ^{*-} final state. For these events, the missing mass of the $K^+\pi^-$ system, $MM(K^+\pi^-)$, was fitted (using a Gaussian shape) at the Λ mass. The missing mass spectra, integrated over all angles and photon energies, are shown in Fig. 1, where the top two plots are for all events and the bottom plots are cut on the Σ^{*-} and Λ final states, respectively. Peaks for the Σ and Σ^* final states are clearly seen in the uncut $MM(K^+)$ spectra (Fig. 1b). The Σ^- decays with nearly

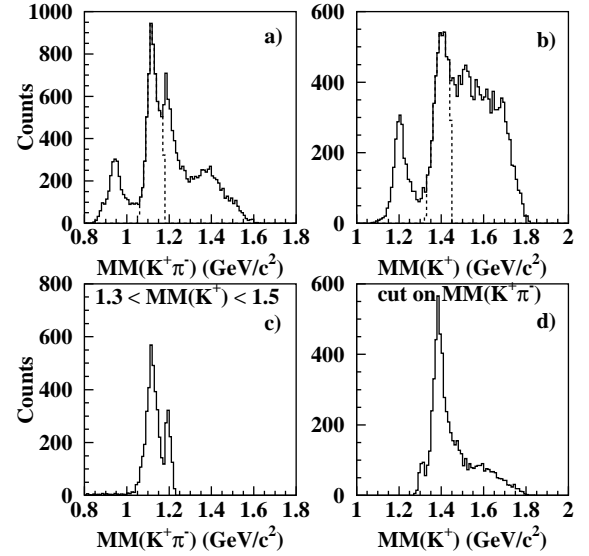


FIG. 1: Mass spectra calculated using the missing mass technique for: (a) detected $K^+\pi^-$; (b) detected K^+ only; (c) same as (a) but cut on the $\Sigma(1385)$ peak shown by the dashed lines in (b); (d) same as (b) but cut on the Λ peak shown by the dashed lines in (a);

100% branching ratio to $n\pi^-$, whereas the Σ^{*-} decays about 87% to $\Lambda\pi^-$ and 11.7% to $\Sigma\pi$.

Peaks at the neutron, Λ and Σ masses are clearly seen in the uncut $MM(K^+\pi^-)$ spectra (Fig. 1a). When a cut on the Σ^{*-} peak is applied (dashed lines in Fig. 1b), the $MM(K^+\pi^-)$ spectra show peaks at both Λ and Σ masses (Fig. 1c). The Σ peak near 1.2 GeV is visible in part due to $\gamma p \rightarrow K^+\Sigma^{*0}$ production followed by the decay $\Sigma^{*0} \rightarrow \Sigma^+\pi^-$.

Similarly, when a cut on the Λ peak is applied (dashed lines in Fig. 1a), the $\Sigma(1385)$ dominates the $MM(K^+)$ spectra (Fig. 1d). The background at higher mass (1.5–1.8 GeV) is due to a combination of high-mass Σ^* states (having greater widths) and some Λ^* resonances produced from the proton, then decaying to the $\Sigma^+\pi^-$. Simulations show that the detector acceptance of the Λ^* (after smearing for Fermi motion) is much smaller in the region of interest than that of the Σ^{*-} .

In the final analysis, a data cut was also applied to remove the small K^{*0} peak in the invariant mass of the $K^+\pi^-$ system (not shown). The K^* production kinematics did not overlap with the Σ^{*-} kinematics due to the forward angle detection of both decay particles in the LEPS spectrometer.

Background from π^+ particles that were misidentified as a K^+ was eliminated by calculating the missing mass $MM(\pi^+\pi^-)$ and then removing those events with $MM(\pi^+\pi^-)$ at the nucleon mass.

The complete set of event selections is: $MM(K^+\pi^-)$

around the Λ peak; $M(K^+\pi^-)$ not at the K^{*0} peak; and $MM(\pi^+\pi^-)$ above the nucleon mass.

Other background from the proton contribution in the deuterium target (*e.g.* due to higher-mass resonance decays) in the region of interest was measured with a liquid hydrogen target. This background (about 20% of the signal) was directly subtracted.

The mass spectra are divided up into nine E_γ bins from 1.5 to 2.4 GeV, and four bins in the kaon center-of-mass angle, θ_{cm} . Counts for both Σ^- and Σ^{*-} final states were extracted by peak fits. The Σ^- peak had extremely little background (after a cut on the neutron peak in the $MM(K^+\pi^-)$ spectrum). After subtracting background from the hydrogen target, the Σ^{*-} decay to $\Lambda\pi^-$ was separated from the background leading to $\Sigma^0\pi^-$ (as shown in Fig. 1c) by fitting to a Gaussian with a fixed mass and a fixed width (extracted from Monte Carlo simulations). The systematic uncertainty in peak fitting is estimated at 7-8% in each bin based on various peakshapes and polynomials used for the background shape. The fitted χ^2 was normally distributed and centered near unity.

Monte Carlo simulations were carried out using the GEANT based [10] *g3leps* software [9]. Events for final states of $K^+\Sigma^{*-}$, $K^+\Sigma^{*0}$, $K^+\Sigma^-$ and $K^+\Lambda(1520)$ from a deuteron target were generated. A realistic beam distribution on target was used, along with known detector resolutions. Fermi broadening of the initial state nucleon in deuterium was done by using the Paris potential. The photon beam energy was calculated from Compton backscattering kinematics, smeared by the energy width of the stored electron beam. Over 10 million events were generated into the detector acceptance, giving hundreds of events for each final state in each of the energy-angle bins. The event generators assumed a flat angular distribution in the center-of-mass frame, which is justified in the end because of the nearly flat angular dependence of the data. The counts from peak fits in each bin were divided by the detector acceptance from the Monte Carlo simulations, typically between 2% to 9% (depending on the bin), giving the unnormalized yield.

The normalization of the data used several factors (see Ref. [9] for details of the procedures). The 16 cm LD₂ target had 6.77×10^{23} deuterons/cm². The tagger detected about 4.0×10^{12} photons, distributed in energy as expected from Compton scattering from the three UV-laser lines. Because of material between the scattering point and the target [9], only $52.6\% \pm 3\%$ of these photons were transmitted to the target. A self-consistent cross check was done by comparing to previously published differential cross sections for the $\gamma n \rightarrow K^+\Sigma^-$ reaction [11], which agreed to within 5%, and is taken as the systematic uncertainty in the acceptance.

Using this normalization, the yield for Σ^{*-} production from the neutron (including the 87% branching ratio for decay to $\Lambda\pi^-$) was converted to the cross sections shown in Fig. 2. The cross sections are, in general, nearly con-

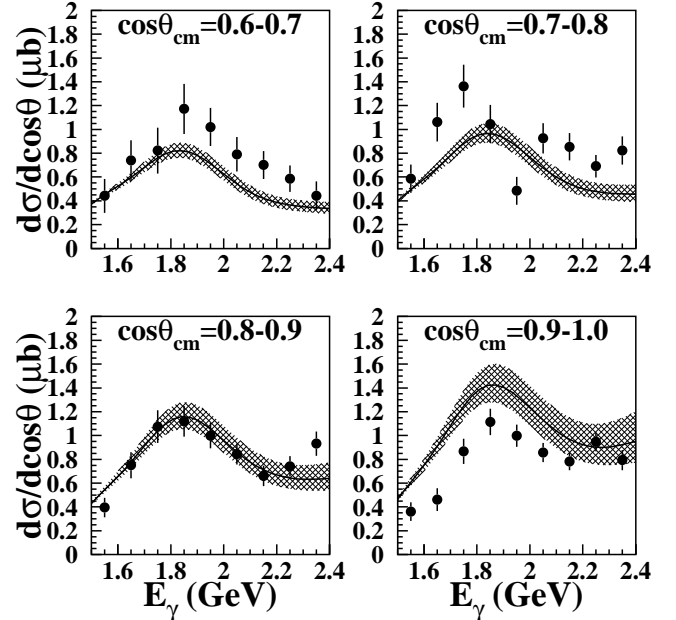


FIG. 2: Cross sections for the reaction $\gamma n \rightarrow K^+\Sigma^{*-}$ as a function of photon energy. Each plot is for the angle bin in $\cos\theta_{cm}$ as shown. The curve is from the model of Ref. [5] and the shaded region extends over the given angular range.

stant for a given photon energy as a function of θ_{cm} . As a function of photon energy, the cross sections initially rise, peaking at about 1.85 GeV, then fall slightly. The cross sections are, on average, slightly smaller than those for Σ^- production at the same angles [11].

Systematic uncertainties are dominated by the peak fits and the background subtraction (from the proton), giving an overall systematic uncertainty of 12%.

Theoretical calculations by Oh, Ko and Nakayama [5] are also shown in Fig. 2 by the solid lines that are obtained by using the phototransition amplitude of resonances from the neutron as predicted in Ref. [7]. The data are in reasonable agreement with the model, but have an angular dependence that is less steep than for the calculations. In the model of Ref. [5], the cross sections at forward angles are dominated by K^+ exchange in the *t*-channel, and the contribution from K^* exchange is negligible. Since K^* exchange makes a strong contribution to the $\gamma p \rightarrow K^+\Lambda$ reaction, the inferred lack of K^* exchange here will allow greater sensitivity to the *s*-channel diagrams in the model of Ref. [5]. Further theoretical investigations of N^* resonances that couple to this channel are desired.

Another independent constraint on the theoretical models is given by the photon beam asymmetry, Σ . For the present results, the beam is linearly polarized, ranging from about 60% at the lowest energy up to $\sim 96\%$ at the Compton edge. The beam asymmetries can be

extracted from the dependence of the cross section on the azimuthal angle, ϕ , as shown in Fig. 3. The beam asymmetry is defined as

$$P_\gamma \Sigma \cos 2\phi = \frac{xN_v - N_h}{xN_v + N_h} \quad (1)$$

where P_γ is the magnitude of the beam polarization, N_v and N_h are the acceptance-corrected counts for the beam polarized vertically and horizontally, respectively, and x is a normalization factor to account for the ratio of luminosity between the two beam polarizations ($x = 0.975 \pm 0.02$ for this analysis). The angle ϕ is measured between the horizontal plane and the reaction plane. Contamination from background was removed using the same procedure as described in Ref. [9]. The systematic uncertainty associated with removal of the background beam asymmetry is only a few percent.

Results for both Σ^- and Σ^{*-} final states are shown, for 3 bins in energy (averaged over all angle bins). Superimposed are curves fit to the expected $\cos 2\phi$ shape. The fit reproduces the data well, where only the amplitude is allowed to vary. The beam asymmetries are clearly much larger for Σ^- than for Σ^{*-} production, and even changes sign. Since asymmetries may be sensitive to the structure of the production amplitudes, the observed small asymmetries constrains the main production mechanism. It is possible that there are multiple contributions to the reaction mechanism (e.g., several s -channel resonances).

The amplitude for the fits shown in Fig. 3, when divided by P_γ for the given photon energy bin, gives the linear beam asymmetry, Σ , as shown in Fig. 4. The large energy bins are necessary in order to get sufficient statistics for the fits shown in Fig. 3. Fits with smaller photon energy bins were also carried out, and no significant energy dependence was seen. For the Σ^- final state, the beam asymmetries are in good agreement with the angle-averaged values measured in Ref. [11] shown by the open points. The beam asymmetries for the Σ^{*-} final state clearly have opposite sign from that of the Σ^- . It also shows a weak energy dependence, although more statistics are desirable to reach a firm conclusion. The systematic uncertainty in the beam asymmetries is about 5%, primarily due to uncertainty measured for the laser polarization.

In contrast to the large values of the beam asymmetry for Σ^- photoproduction predicted by the KaonMAID model [12], the Σ^{*-} production model of Ref. [5] predicts very small beam asymmetries. It was suggested in Ref. [5] that the beam asymmetry is sensitive to the presence of s -channel resonance contributions for Σ^{*0} photoproduction, switching from slightly positive for no resonances to slightly negative when all resonance contributions are included (note the change in sign in the definition of beam asymmetry for Ref. [5]). Calculations in this theoretical model are shown for the present reaction (for Σ^{*-}) by the solid line in Fig. 4. These calculations

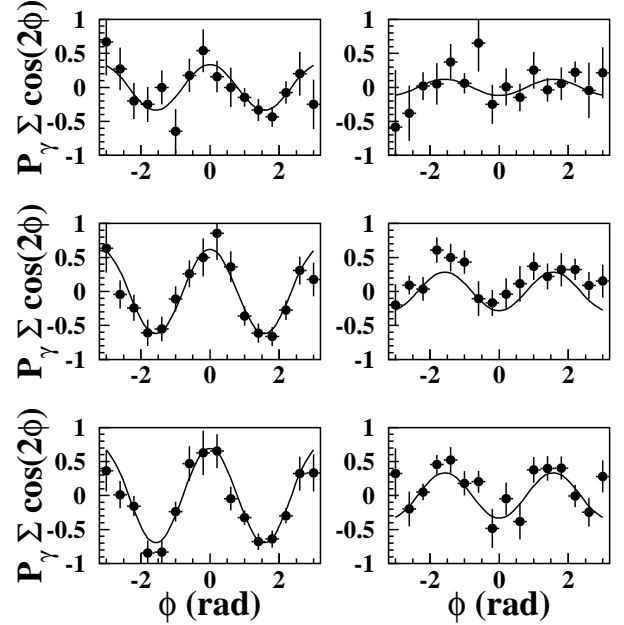


FIG. 3: Azimuthal angle ϕ -dependence of the asymmetry given by Eq. (1) for $K^+\Sigma^-$ (left) and $K^+\Sigma^{*-}$ (right) photoproduction from the deuteron. Three energy bins are shown: 1.5-1.8 GeV (top), 1.8-2.1 GeV (middle) and 2.1-2.4 GeV (bottom). The curves are fit to the function $A \cos 2\phi$.

have been averaged over the same angular range as for the current experiment. In the model of Ref. [5], the K^* exchange gives a large asymmetry, as large as 0.5 at $\cos \theta_{cm} \simeq 0.5-0.8$ and $E_\gamma \leq 2.4$ GeV. Therefore, a small beam asymmetry suggests that K^* exchange is somewhat suppressed. However, the discrepancy between the theoretical curve and the data in Fig. 4 requires further theoretical studies.

In general, the experimental values are consistently more negative than the theoretical predictions over the entire photon energy range of 1.5-2.4 GeV, which are near to zero for the whole integrated angular range. It is possible that final-state interactions in the deuteron target could change the theoretical calculations, and since the predicted beam asymmetry is small, these effects could be significant. The present data will serve to constrain future improvements in the theoretical calculations.

In summary, we have measured the first photoproduction cross sections and beam asymmetries for $K^+\Sigma^{*-}$ photoproduction from the deuteron, by detecting both a K^+ and π^- in the final state using the LEPS spectrometer. The measurement is limited to forward angles ($\cos \theta_{cm} > 0.6$) and photon energies of 1.5-2.4 GeV. Simultaneously, Σ^- photoproduction was measured and shows good agreement with previous data [11]. The cross sections for Σ^{*-} photoproduction peak at about 1.85 GeV and show a nearly-flat angular distribution. The

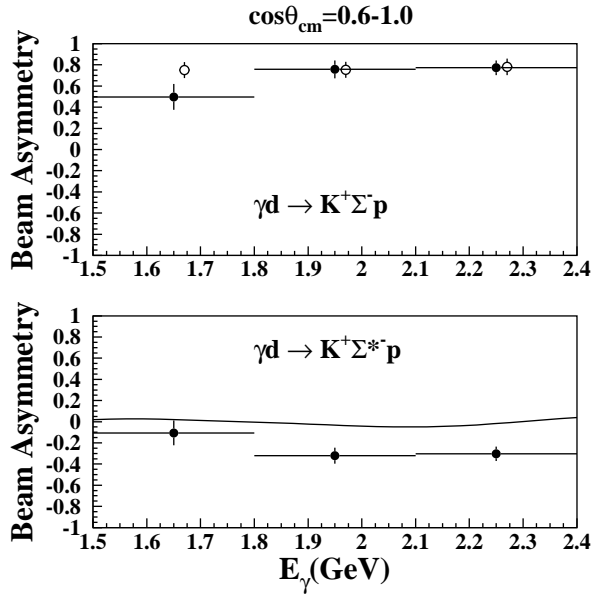


FIG. 4: Linear beam asymmetry, Σ , for the reactions $K^+ \Sigma^-$ (top) and $K^+ \Sigma^{*-}$ (bottom) photoproduction from the deuteron as a function of photon energy. The open points in the top plot are weighted averages from Ref. [11], which are offset from the bin center for visibility. The curve is from the model of Ref. [5].

beam asymmetries are small and negative, and comparison with calculations in the model of Ref. [5] may suggest that there are multiple s -channel resonance contributions to Σ^{*-} photoproduction, and that K^* exchange in the t -channel is largely absent. These data may also be useful to constrain other theoretical calculations of Σ^{*-} photoproduction, such as in the model of Lutz and Soyer [13], and will be explored in a future paper.

The authors gratefully acknowledge the contributions of the staff at the SPring-8 facility. This research was supported in part by the US National Science Foundation, the Ministry of Education, Science, Sports and Culture of Japan, the National Science Council of the Republic of China, and the KOSEF of the Republic of Korea.

-
- [1] J.H.R. Crouch *et al.*, Phys. Rev. **156**, 1426 (1967); R. Erbe *et al.*, Nuovo Cimento **49A**, 504 (1967); R. Erbe *et al.*, Phys. Rev. **188**, 2060 (1969); K. Abe *et al.*, SLAC-PUB-3634, 1985.
 - [2] L. Guo and D.P. Weygand, *Proceedings of the International Workshop on the Physics of Excited Baryons* (NSTAR05), S. Capstick, V. Crede, and P. Eugenio, eds., pp. 306-309, World Scientific, Singapore, 2006; arXiv:hep-ex/0601010.
 - [3] M. Niiyama *et al.*, Phys. Rev. C **78**, 035202 (2008).
 - [4] F. Close, *An Introduction to Quarks and Partons*, Academic Press, London, 1979.
 - [5] Y. Oh, C.M. Ko, and K. Nakayama, Phys. Rev. C **77**, 045204 (2008).
 - [6] Particle Data Group, J. Phys. G **33**, 1 (2006).
 - [7] S. Capstick and W. Roberts, Phys. Rev. D **58**, 074011 (1998); S. Capstick, Phys. Rev. D **46**, 2864 (1992).
 - [8] M. Döring, E. Oset, and D. Strottman, Phys. Rev. C **73**, 045209 (2006).
 - [9] M. Sumihama *et al.*, Phys. Rev. C **73**, 035214 (2006).
 - [10] CERN Application Software Group, GEANT 3.2, CERN Program Library writeup W5013 (1994).
 - [11] H. Kohri *et al.*, Phys. Rev. Lett. **97**, 082003 (2006).
 - [12] T. Mart *et al.*, KaonMAID (2000); www.kph.uni-mainz.de/MAID/kaon/kaonmaid.html.
 - [13] M.F.M. Lutz and M. Soyeur, Nucl. Phys. **A748**, 499 (2005).